

000 BEYOND INVARIANCE: A FEATURE-STRENGTH PER- 001 002 SPECTIVE FOR OOD GENERALIZATION 003 004

005 **Anonymous authors**

006 Paper under double-blind review

007 ABSTRACT

011 Out-of-Distribution (OOD) generalization is a central challenge in machine learning.
 012 Models often fail on unseen data, not because of an inability to learn robust
 013 signals, but because they *preferentially learn spurious, dataset-specific correlations* that are *highly predictive for in-distribution examples*. Existing solutions
 014 typically focus on searching for invariant features, yet often overlook a more fundamental question: **what properties of the training data cause models to learn**
 015 **these non-invariant “shortcut” features in the first place?** In this work, we
 016 present a different perspective on OOD generalization. We argue that failures to
 017 generalize are a direct consequence of models learning the strongest features in the
 018 training data, which are often spurious. Guided by this, we reframe OOD generalization
 019 not as a search for invariance, but as the *problem of identifying and mitigating the influence of these overly dominant features*. Under this new perspective,
 020 we develop a novel primitive for quantifying feature strength across a training
 021 set. This primitive gives rise to a targeted regularization algorithm that weakens a
 022 model’s reliance on the identified strongest features, thereby compelling it to learn
 023 more robust and causally stable signals. Our method demonstrates substantial im-
 024 provements in generalization across a wide range of OOD benchmarks, improving
 025 OOD accuracy by up to $2\times$ over standard training and significantly outperforming
 026 existing baselines without compromising in-distribution performance.
 027

029 1 INTRODUCTION

031 A central goal of machine learning is to build
 032 models that generalize beyond their training
 033 data. Yet, the standard paradigm of minimizing
 034 empirical risk often fails precisely at this task,
 035 especially when faced with Out-of-Distribution
 036 (OOD) data (Beery et al., 2018; Ben-David
 037 et al., 2010; Bengio et al., 2019; DeGrave et al.,
 038 2020; Moreno-Torres et al., 2012; Recht et al.,
 039 2019; Taori et al., 2020). Models that achieve
 040 high in-distribution accuracy frequently do so
 041 by exploiting spurious correlations, *i.e.*, “short-
 042 cut” features (Geirhos et al., 2020; Pezeshki
 043 et al., 2021) that are highly predictive within
 044 the training set but fail to hold in new envi-
 045 ronments. A model trained to classify cows,
 046 for instance, might learn to recognize pastures
 047 rather than the animal itself; a medical diagnos-
 048 tic tool might rely on hospital-specific markings
 049 instead of the underlying pathology. These failures are not exceptions, but a common consequence
 050 of training powerful models on finite, biased datasets.

051 The prevailing perspective on mitigating such failures is to frame OOD generalization as a search
 052 for invariance. This approach, rooted in principles of causality, seeks to identify and isolate features
 053 whose predictive relationship with the label remains stable across different training environments.
 This perspective is a natural one and has led to a host of methods, including invariant risk mini-
 054 mization (Arjovsky et al., 2019; Ahuja et al., 2020; Koyama & Yamaguchi, 2020; Krueger et al.,



Figure 1: Illustration of spurious feature reliance: models trained with ERM often latch onto the statistically strongest signals (e.g., background water or sand) rather than robust causal features, leading to misclassification under distribution shift.

054 2021; Robey et al., 2021; Zhang et al., 2021a) and distributional matching (Ganin et al., 2016; Li
 055 et al., 2018; Sun & Saenko, 2016). The core assumption is that if a model can be restricted to only
 056 use these stable, invariant features, it will naturally generalize to unseen domains where the spuri-
 057 ous correlations have shifted. However, while the pursuit of invariance is well-motivated, it often
 058 sidesteps a more fundamental question:

059 **(Q)** *Why do models learn spurious, non-invariant features so readily in the first place, even
 060 when robust alternatives exist in the data?*

062 In this work, we take a step back and offer a different perspective on OOD generalization. We
 063 argue that the failures of modern classifiers are not merely an incidental byproduct of training, but
 064 a direct consequence of the learning objective itself, such as Empirical Risk Minimization (ERM)
 065 forces the model to learn the most statistically powerful signals to minimize the training loss, even
 066 if those signals are spurious “shortcuts” that fail to generalize. Models are designed to find the
 067 most predictive signals available (Ahuja et al., 2020; Heinze-Deml et al., 2018; Ahuja et al., 2021),
 068 and in many real-world datasets, the most statistically powerful features are precisely the spurious
 069 ones (see Figure 1). A simple background texture or a watermark, if consistently correlated with a
 070 label, provides a far easier-to-learn signal than the complex, nuanced features that define a class in a
 071 truly robust way. The optimization process, driven by empirical risk minimization, has no inherent
 072 mechanism to distinguish between a causal feature and a coincidental one; it only follows the path
 073 of steepest descent on the training loss.

074 The problem, then, is not simply that non-invariant features exist, but that they are often the strongest
 075 features in the training data; these are easy-to-learn, highly predictive signals that the model prefer-
 076 entially learns to minimize its training error. This reveals a fundamental tension: the very process
 077 designed to achieve high accuracy on the training set may be the primary driver of generalization
 078 failure on OOD data. This observation suggests a reframing of the OOD problem: rather than
 079 searching for invariant features, we should instead focus on identifying the features that are overly
 080 dominant and mitigating their influence. If a model’s reliance on these strong-but-spurious signals
 081 can be weakened, it can be compelled to learn the more subtle, but more robust, features that are
 082 essential for true generalization.

083 Guided by this new perspective, we develop a simple yet effective framework for improving OOD
 084 generalization by directly addressing the influence of dominant features. We first introduce a novel
 085 primitive for quantifying the “strength” of any feature across the training set. This primitive mea-
 086 sures the degree to which the presence of a feature in the training data influences the model’s final
 087 predictions. This naturally gives rise to a detection and regularization algorithm. Our method first
 088 identifies the features with the highest strength scores and, by extension, the training examples that
 089 provide the most support for them. It then applies a targeted regularization that weakens the model’s
 090 dependence on these specific examples. This process discourages the model from overfitting to
 091 the strongest, most obvious correlations and encourages it to learn the causally stable signals that
 092 generalize to new distributions. **In summary**, our contributions are as follows:

- 092 ① We re-frame the problem of OOD generalization as one of detecting and mitigating the
 093 influence of the strongest features in a dataset, which are often spurious. We argue that
 094 generalization failures are a direct consequence of the learning objective itself, which com-
 095 pels models to preferentially learn these dominant, and often spurious, signals over more
 096 robust alternatives.
- 097 ② Based on this new perspective, we introduce a novel primitive for quantifying the “strength”
 098 of any feature across a training set. This primitive enables an algorithm that first identifies
 099 the most dominant features and the training examples that support them, and then applies a
 100 targeted regularization to provably weaken the model’s reliance on these specific examples,
 101 compelling it to learn more causally stable signals.
- 102 ③ We demonstrate the effectiveness of our approach through extensive experiments on OOD
 103 Benchmarks like *Waterbirds*, *Colored MNIST* (Lecun et al., 1998), *CelebA* (Liu et al.,
 104 2015), *Digits*, *PACs* (Li et al., 2017), and *VLCS* (Torralba & Efros, 2011). Our method
 105 achieves substantial gains, increasing OOD accuracy up to 2 \times over standard ERM (Vap-
 106 nik, 1991) and significantly outperforming strong baselines including *IRM* (Arjovsky et al.,
 107 2019), *IB-ERM* (Ahuja et al., 2021), *Group-DRO* (Sagawa et al., 2020), and *CORAL* (Sun
 & Saenko, 2016).

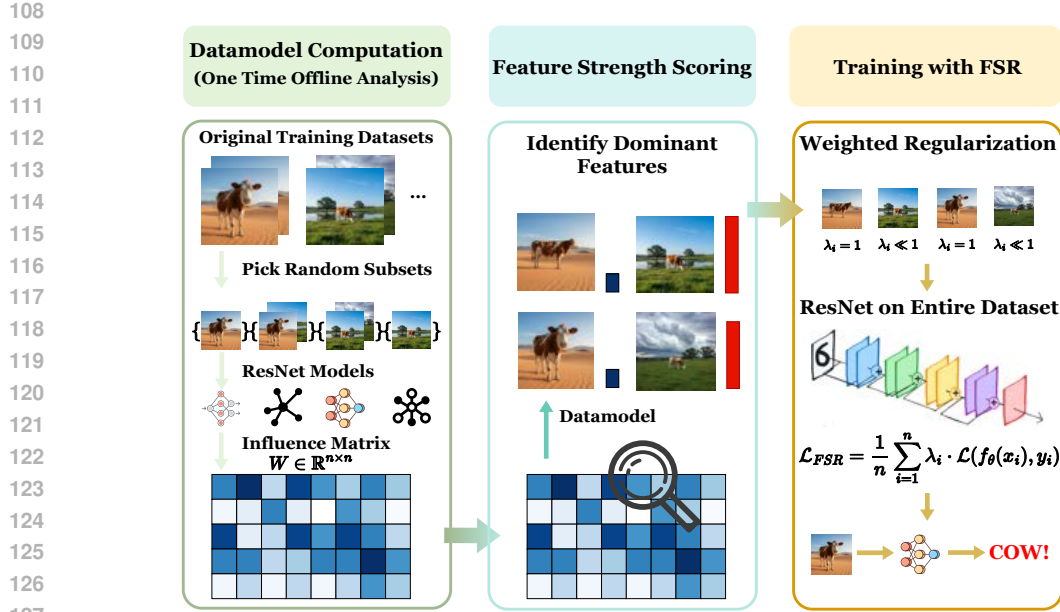


Figure 2: Overview of the proposed Feature Strength Regularization (FSR) framework. The method computes datamodels on random subsets to identify dominant features and applies weighted regularization to reduce reliance on spurious signals, guiding the model toward more robust representations.

2 RELATED WORKS

The problem of OOD generalization has motivated a significant body of research, largely centered on learning models that are robust to shifts between training and test distributions (Liu et al., 2021). A prevailing perspective casts this as a problem of invariance, seeking to isolate features that are causally linked to the label and thus stable across domains. Our work diverges from this tradition by proposing that the root cause of poor generalization lies not just in the existence of spurious features, but in their statistical strength within the training data. One prominent line of work, exemplified by Invariant Risk Minimization (IRM) (Arjovsky et al., 2019), attempts to learn representations that elicit an optimal classifier across multiple training environments. This principle is also explored in various other forms (Ahuja et al., 2020; Krueger et al., 2021; Jiang & Teney, 2024). While IRM and its variants seek to isolate features that are stable across domains, our approach addresses a more fundamental question: why models fail to learn them in the first place. We posit that models preferentially learn the strongest features, regardless of their invariance.

Another set of approaches focuses on feature decorrelation through sample reweighting, as seen in StableNet (Zhang et al., 2021b). By reweighting training samples, this method aims to remove statistical dependencies between all features, thereby preventing the model from capturing spurious correlations that arise from these dependencies. Other methods also pursue feature decorrelation through different mechanisms, such as moment matching or explicit regularization (Sun & Saenko, 2016; Peng et al., 2019). However, in our approach, instead of decorrelating all features, we identify and specifically regularize against only the strongest ones, which we hypothesize are the primary drivers of generalization failure. More recent work has explored the connection between the Information Bottleneck (IB) principle and OOD generalization (Ahuja et al., 2020). These methods propose that by compressing the input representation as much as possible while retaining information about the label, a model can be encouraged to discard non-essential, spurious features that may not generalize. Distributionally Robust Optimization (DRO) offers another perspective, optimizing for worst-case performance over a set of plausible test distributions (Sagawa et al., 2019). By defining an uncertainty set around the training distribution, often using measures like Wasserstein distance (Mohajerin Esfahani & Kuhn, 2018), DRO aims to learn a model that is robust to shifts within this set, often leading to improved worst-group accuracy. Another related area focuses on feature selection, often framed as identifying a minimal set of variables that are causally stable predictors of the label, such as Markov boundary (Bhattacharyya et al., 2023). These methods aim to explicitly separate causal features from non-causal or inactive ones (Zhang et al., 2025).

162 While these methods offer different mechanisms for improving generalization, they all share a com-
 163 mon focus: they attempt to either find invariant features or mitigate the effects of domain-specific
 164 ones. They do not, however, directly address the question of why certain spurious features are
 165 learned so readily, nor do they provide a primitive for quantifying the influence of specific training
 166 examples on this process. Our work diverges from this tradition by proposing that the root of poor
 167 OOD generalization lies not just in the existence of spurious features, but in their strength, and we
 168 offer a direct mechanism to identify and counteract their influence. For a detailed discussion on
 169 related works, please refer to Appendix B.

171 3 PROPOSED METHOD: FEATURE STRENGTH REGULARIZATION (FSR)

173 Our method (summarized in Figure 2) is built on the premise that OOD generalization failures are
 174 caused by models over-relying on the statistically strongest features in the training data. We first for-
 175 malize this problem setting, then introduce a primitive to quantify said feature strength, and finally
 176 present our algorithm for feature-strength regularization, along with its theoretical justification.

177 3.1 PRELIMINARIES

179 We consider a standard supervised learning setup where our input space is $\mathcal{Z} = \mathcal{X} \times \mathcal{Y}$. We
 180 are given a training dataset $\mathcal{S} = \{(x_i, y_i)\}_{i=1}^n$ of size n , with each example (x_i, y_i) drawn i.i.d.
 181 (Independent and Identically Distributed) from a training distribution P_{tr} . The goal is to train a
 182 model f_θ , parameterized by weights θ , using a learning algorithm \mathcal{A} that generalizes to an unseen
 183 test distribution P_{te} , where $P_{te} \neq P_{tr}$.

184 The standard approach is Empirical Risk Minimization (ERM), which seeks to find parameters θ^*
 185 that minimize the average loss on the training set:

$$187 \theta^* = \arg \min_{\theta} \frac{1}{n} \sum_{i=1}^n \mathcal{L}(f_\theta(x_i), y_i) \quad (1)$$

189 where \mathcal{L} is a loss function. The fundamental problem in OOD generalization is that minimizing
 190 this empirical risk often leads to solutions that learn spurious correlations to P_{tr} , resulting in poor
 191 performance on P_{te} . This happens because ERM is agnostic to the causal structure of the data and
 192 will readily exploit any statistically predictive pattern to minimize \mathcal{L} , regardless of its robustness.

194 3.2 A PRIMITIVE FOR QUANTIFYING FEATURE STRENGTH

196 Our core hypothesis is that this failure is driven by the model’s tendency to rely on the statistically
 197 strongest features. To formalize this, we build on the framework of [Khaddaj et al. \(2023\)](#).

198 **Definition 1 (Feature and Support).** A feature is a function $c : \mathcal{X} \rightarrow \{0, 1\}$
 199 that indicates the presence of an arbitrary property in an input. This allows us
 200 to group examples based on shared characteristics, such as “contains grass”
 201 (c_{grass}) or “is a nighttime photo” (c_{night}). The support set of a feature c in a
 202 dataset S , denoted S_c , is the subset of examples where the feature is present:
 203 $S_c = \{(x, y) \in S \mid c(x) = 1\}$.

204 Based on this, we propose that a feature’s “strength” is its marginal contribu-
 205 tion to the model’s performance. A feature is strong if including examples
 206 that contain it provides a powerful, easily learned signal for minimizing the
 207 training loss. We thus formally define feature strength below:

208 **Definition 2 (Feature Strength).** Let \mathcal{D}_S be a distribution over subsets of
 209 training data S . The k -conditional performance of a feature c , denoted $V_c(k)$,
 210 is the model’s expected performance on examples from the support set S_c ,
 211 conditioned on being trained with a subset $S' \subset S$ that contains exactly k
 212 examples from S_c :

$$213 V_c(k) = \mathbb{E}_{z \sim S_c} [\mathbb{E}'_{S' \sim \mathcal{D}_S} [f(z; S') \mid |S'_c| = k, z \notin S']] \quad (2)$$

215 where $f(z; S')$ is a performance metric (e.g., classification margin) on example z for a model trained
 on S' .



Figure 3: Some examples of the original and the patched images used for training.

216 The *k*-marginal influence of the feature, denoted $I_c(k)$, is the marginal gain in performance from
 217 adding one additional example of the concept to the training set:

$$I_c(k) = V_c(k+1) - V_c(k) \quad (3)$$

221 A feature is considered “strong” if its marginal influence $I_c(k)$ is consistently high and positive.
 222 This means that each additional example of the feature provides a significant boost to the model’s
 223 performance on that feature, indicating that the model is effectively learning the association.

224 **Intuitive Example (Cows on Grass).** Consider a dataset where most images of **cows** are in
 225 **grass** backgrounds. We have a robust feature, c_{cow} (“contains a cow”), and a spurious one,
 226 c_{grass} (“has a grass background”). Because the grass texture is a simple, low-level feature
 227 that is highly correlated with the **cow** label in the training data, the model can quickly learn
 228 the shortcut **grass** → **cow**. Thus, the *k*-marginal influence of the **grass** feature, $I_{grass}(k)$, will
 229 be very high for a small k . In contrast, learning the complex, varied characteristics of a **cow**
 230 is harder. The *k*-marginal influence of the **cow** feature, $I_{cow}(k)$, will be positive but smaller.
 231 The model, driven by ERM, follows the path of steepest descent and preferentially learns the
 232 stronger, spurious feature.

233 This leads to our central assumption:

234 **Assumption 1 (The Strongest Feature Hypothesis).** Let c_s be a spurious concept and c_r be a
 235 robust, causal feature. In a biased training set, the spurious feature is often statistically stronger, *i.e.*,
 236 $I_{c_s}(k) > I_{c_r}(k)$ for relevant values of k . A model trained with ERM will preferentially learn c_s at
 237 the expense of c_r , leading to poor OOD performance.

238 3.3 EMPIRICAL VALIDATION OF THE STRONGEST FEATURE HYPOTHESIS

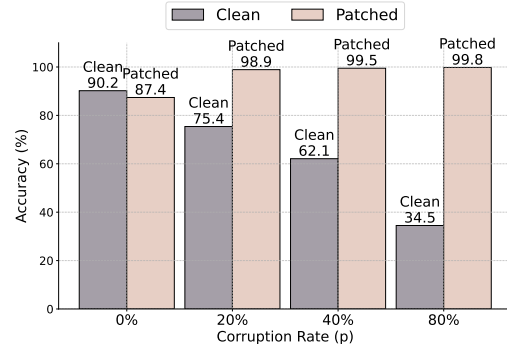
239 Before introducing our algorithm, we provide
 240 empirical evidence for our central hypothesis:
 241 that models trained with ERM are biased towards
 242 learning the strongest available statistical signals,
 243 even when those signals are spurious.

244 **Experimental Setup.** We conduct a controlled
 245 experiment on CIFAR-10 (Krizhevsky, 2009).
 246 We introduce a synthetic, spurious feature, a
 247 small 6×6 (36 pixels) bright green square, into
 248 a fraction p of the training images belonging to
 249 a single target class: *airplane*. This class was
 250 chosen because its typical background (blue/gray
 251 sky) ensures the green patch is a distinctly non-
 252 causal feature. Some examples of this augmenta-
 253 tions are shown in Figure 3. This patch becomes
 254 a “shortcut”: a statistically powerful but causally irrelevant signal for the airplane class. We train a
 255 standard ResNet-18 (He et al., 2016) model and vary the corruption rate of $p \in \{0, 10, 20, 40, 80\}\%$.
 256 We measure two metrics: (i) accuracy on clean test images of airplanes, and (ii) accuracy on test
 257 images of airplanes with the green patch added.

258 **Results.** The results, summarized in Figure 4, provide clear evidence of our hypothesis. As the
 259 green patch becomes more prevalent, its statistical strength increases. The ERM-trained model
 260 increasingly relies on this simple shortcut, leading to a collapse in its ability to recognize genuine
 261 airplanes without the patch. This experiment demonstrates that the strongest feature, when spurious,
 262 is not just learned; it is learned at the expense of more robust features. This directly motivates an
 263 algorithmic intervention to mitigate the influence of such dominant features.

264 3.4 ALGORITHM: FEATURE STRENGTH REGULARIZATION (FSR)

265 Our goal is to develop an algorithm that identifies the strongest features and regularizes the model
 266 to reduce its dependence on them.



267 Figure 4: As the prevalence of the spurious green
 268 patch increases, the model’s accuracy on clean air-
 269 planes drops precipitously, while its accuracy on
 270 patched airplanes remains near-perfect.

270 **Estimating Feature Strength.** While Definition 2 provides a formal way to conceptualize feature
 271 strength, its direct computation is intractable. It would require training an exponential number of
 272 models on different subsets of the data to estimate the conditional expectations accurately. To make
 273 this estimation feasible, we leverage the datamodels framework (Ilyas et al., 2022). Datamodels
 274 provide an efficient linear approximation for a model’s output on a test example z as a function of
 275 the training subset S' it was trained on:

$$\mathbb{E}[f(z; S')] \approx \mathbb{1}_{S'}^\top w_z \quad (4)$$

276 where $\mathbb{1}_{S'}$ is the indicator vector of subset S' and $w_z \in \mathbb{R}^n$ is a vector of influence weights. The
 277 ability of this framework to accurately capture the model’s behavior is critical to our method, which
 278 we state as an explicit assumption.

281 **Assumption 2 (Datamodel Accuracy).** For any example z , with a corresponding datamodel weight
 282 vector $w_z \in \mathbb{R}^n$, the expected squared error of the linear approximation is bounded:

$$\mathbb{E}_{S' \sim \mathcal{D}_S} [(\mathbb{E}[f(z; S')] - \mathbb{1}_{S'}^\top w_z)^2] \leq \epsilon \quad (5)$$

285 where $\epsilon > 0$ is the bound on the error of estimating the model output function using datamodels.

286 Assumption 2 guarantees that the complex, non-linear behavior of a deep neural network can be
 287 reliably approximated by a simple linear model over training subsets. As shown by Khaddaj et al.
 288 (2023), under this assumption, the marginal influence $I_c(k)$ from Equation 3.2 can be estimated in
 289 a closed form using pre-computed datamodel weights $\{w_z\}_{z \in S}$.

290 **The FSR Algorithm.** Our algorithm proceeds in three-stages:

- 292 **① Datamodel Computation:** This is a one-time, upfront cost. We train a large number of
 293 models on a random subsets of the training data to compute the influence matrix $W \in \mathbb{R}^{n \times n}$, where the i -th row is the weight vector $w_{z_i}^T$.
- 295 **② Feature Strength Scoring:** For a predefined set (essentially represented by the random
 296 subsets) of candidate features, we use the datamodels to estimate their strength. We then
 297 assign a score to each training example x_i by aggregating the strengths of all features it
 298 possesses.
- 299 **③ Weighted Regularization:** We modify the ERM objective to down-weight examples with
 300 high strength scores. The *Feature Strength Regularization* (FSR) objective is:

$$\mathcal{L}_{FSR} = \frac{1}{n} \sum_{i=1}^n \lambda_i \cdot \mathcal{L}(f_\theta(x_i), y_i) \quad (6)$$

304 where $\lambda_i \in [0, 1]$ is a weight inversely proportional to the strength score of example x_i .
 305 This discourages the model from relying on the strongest signals, forcing it to learn from a
 306 wider and more robust set of features.

3.5 THEORETICAL JUSTIFICATION.

310 Our regularization scheme is justified by the fact that our strength estimation primitive can provably
 311 identify the examples that support the strongest feature. This identification can be framed as a
 312 combinatorial optimization problem.

314 3.5.1 APPROXIMATING THE STRONGEST FEATURE SET

316 The task of identifying the strongest feature can be framed as a combinatorial optimization problem.
 317 Let W be the datamodel influence matrix. The task of finding the feature c with support size $p = |S_c|$
 318 that has the greatest strength can be shown to be equivalent to finding an indicator vector $v \in \{0, 1\}^n$
 319 with $\|v\|_1 = p$ that maximizes a quadratic form. Let $h(v) = \frac{1}{\|v\|_1} v - \frac{1}{n - \|v\|_1} (1_n - v)$ be a vector
 320 that contrasts the average influence from within the set indicated by v against the average influence
 321 from outside it. The optimization problem is:

$$\max_{v \in \{0,1\}^n, \|v\|_1=p} \sum_{i: v_i=1} \left(W_i v - \frac{p}{n-p} W_i (1_n - v) \right) = \max_{v \in \{0,1\}^n, \|v\|_1=p} v^\top \left(W - \text{diag} \left(\frac{p}{n-p} W 1_n \right) \right) v$$

324
 325 Table 1: Test accuracies (%) on Waterbirds, ColoredMNIST, and CelebA in the *unbalanced* setting
 326 using ResNet9 as the backbone. We report both the average OOD accuracy (OOD Avg.) and the
 327 worst-group accuracy (OOD Worst) for each dataset. Best results per column are shown in **bold**.

Methods	Waterbirds		ColoredMNIST		CelebA	
	OOD Avg. \uparrow	OOD Worst \uparrow	OOD Avg. \uparrow	OOD Worst \uparrow	OOD Avg. \uparrow	OOD Worst \uparrow
Random Subset (50%)	74.5%	37.9%	14.7%	0.0%	69.0%	26.8%
CRAIG (Core-Set)	89.4%	48.9%	25.7%	0.0%	88.3%	40.2%
ERM	91.5%	55.9%	26.7%	0.0%	90.4%	46.8%
IRM	84.3%	63.8%	69.9%	64.0%	90.1%	74.1%
IB-IRM	85.4%	64.3%	70.0%	64.3%	89.5%	78.0%
Group-DRO	86.8%	86.1%	70.2%	63.5%	89.1%	78.4%
CORAL	86.2%	66.0%	69.7%	64.1%	90.1%	74.0%
FSR (Ours)	90.4%	89.4%	71.5%	64.1%	90.7%	78.4%

336 While this maximum-sum submatrix problem is NP-hard, its solution corresponds to the set of ex-
 337 amples supporting the strongest feature. Given the intractability of an exact solution for large n , we
 338 do not solve this problem exhaustively. Instead, we employ a scalable heuristic to find an approxi-
 339 mate solution. Specifically, we use a greedy local search algorithm inspired by the Kernighan-Lin
 340 heuristic (Kernighan & Lin, 1970), which iteratively swaps elements to improve the objective func-
 341 tion. While this approximation does not come with formal error bounds, it is empirically effective
 342 at identifying influential data subsets (Khaddaj et al., 2023).

3.5.2 THEORETICAL GUARANTEES

344 Our approach is grounded in two key theoretical results. The first establishes that our primitive
 345 correctly identifies the strongest feature set, while the second guarantees that regularizing against
 346 this set improves OOD generalization compared to standard ERM.

347 **Theorem 1 (Feature Identification).** Let c_p be the strongest feature in the dataset with support
 348 size p . Under Assumption 1 (Strongest Features Impede Generalization) and Assumption 2 (Data-
 349 model Accuracy), the unique maximizer of the optimization problem above is the indicator vector
 350 $v_p = \mathbb{1}_{S_{c_p}}$ for the support set of c_p , provided the strength gap between c_p and any other feature is
 351 sufficiently large.

352 **Proof Sketch.** We provide a full proof in Appendix C. The proof proceeds in two main steps. (i) By
 353 Assumption 1, the strongest feature c_p has a higher true strength than any other feature. (ii) If the
 354 approximation error from the datamodel (bounded by Assumption 2) is smaller than this strength
 355 gap, the maximizer of our objective must correspond to the indicator vector for the strongest feature.

356 This theorem provides theoretical grounding to our approach. It confirms that by solving (or ap-
 357 proximating the solution to) this optimization problem, we can identify the training examples that
 358 are the primary source of a model’s reliance on spurious features.

360 **Theorem 2 (Generalization Improvement of FSR over ERM).** Let c_s be the strongest feature,
 361 which is spurious (*i.e.*, its correlation with the label y changes from P_{tr} to P_{te} , and let c_r be a
 362 weaker, robust feature whose correlations with y is stable across P_{tr} and P_{te} . Under Assumptions 1
 363 and 2, the expected OOD risk of FSR is lower than that of ERM:

$$\mathbb{E}_{P_{te}} [\mathcal{L}_{FSR}] < \mathbb{E}_{P_{te}} [\mathcal{L}_{ERM}] \quad (7)$$

366 **Proof Sketch.** The full proof is provided in Appdendix D. The intuition is that ERM, by definition,
 367 learns a predictor f_{ERM} that relies heavily on the strongest feature, c_s . Because this feature is
 368 spurious, f_{ERM} will incur high risk on the test distribution P_{te} . In contrast, FSR identifies the
 369 examples supporting c_s and down-weights their contribution to the loss. This forces the optimizer to
 370 learn from the remaining signals, including the weaker but robust feature c_r . The resulting predictor,
 371 f_{FSR} relies less on c_r , leading to a lower expected risk on P_{te} .

373 4 EXPERIMENTS

375 4.1 EXPERIMENTAL SETUP

377 **Datasets.** We evaluate our approach on a diverse suite of seven OOD benchmarks, covering a va-
 378 riety of distribution shifts: **(1) Spurious Correlation:** We use Waterbirds, Colored MNIST (Lecun

378 et al., 1998), and CelebA (Liu et al., 2015), which are specifically designed to have strong spurious
 379 correlations between the background or color and the class label. **(2) Domain Shift:** We use
 380 PACS (Li et al., 2017), and VLCS (Torralba & Efros, 2011), which contain images from different
 381 domains (e.g., photo, sketch, cartoon) and are standard for evaluating domain generalization. **(3)**
 382 **Subpopulation Shift:** We use Digits dataset, which involves shifts in writing styles. For detailed
 383 information for each dataset, please refer to Appendix E.

384 **Baselines.** We compare FSR against a set of strong and widely-used baselines: **(1) Straw-**
 385 **man Baselines:** Random Set, and CRAIG (Mirzasoleiman et al., 2020) (Core-set selection). **(2)**
 386 **OOD Baselines:** Empirical Risk Minimization (ERM) (Vapnik, 1991), Invariant Risk Minimization
 387 (IRM) (Arjovsky et al., 2019), Information Bottleneck IRM (IB-IRM) (Ahuja et al., 2021), Group
 388 Distributionally Robust Optimization (Group-DRO) (Sagawa et al., 2020), and CORAL (Sun &
 389 Saenko, 2016). For more information on each of these methods please refer to Appendix F.

390 **Implementation Details.** For experiments on Colored MNIST and Colored FMNIST, we simply
 391 use an MLP with 1 hidden layer with 128 units. For all other datasets we use a ResNet-9 (He et al.,
 392 2016), pretrained on ImageNet Deng et al. (2009) as backbone. For the detailed parameters and
 393 settings, refer to Appendix G.

394 Table 2: Results of the *unbalanced* setting on PACS and VLCS using ResNet9 pretrained on Image-
 395 Net as backbone. Numbers are test accuracies (%). Best per column in **bold**.

	PACS					VLCS				
	Art.	Cartoon	Sketch	Photo	Avg.	Caltech	Labelme	Pascal	Sun	Avg.
Random Subset (50%)	60.7%	59.3%	53.1%	81.8%	63.7%	85.9%	51.7%	50.8%	40.1%	57.1%
CRAIG (Core-Set)	62.9%	61.1%	54.8%	83.0%	65.5%	87.1%	52.6%	52.3%	41.5%	58.4%
ERM	68.2%	66.1%	60.5%	87.0%	70.5%	89.4%	55.1%	57.2%	46.0%	61.9%
IRM	66.8%	64.9%	59.6%	86.1%	69.4%	88.6%	54.7%	56.4%	45.3%	61.3%
IB-IRM	69.1%	65.7%	61.2%	86.6%	70.7%	89.0%	58.9%	58.1%	49.8%	64.0%
Group-DRO	69.5%	66.4%	65.3%	87.1%	72.1%	89.8%	55.9%	60.9%	47.0%	63.4%
CORAL	73.2%	68.0%	63.8%	88.4%	73.4%	91.6%	57.4%	59.5%	48.1%	64.2%
FSR (Ours)	72.6%	70.5%	64.5%	89.2%	74.2%	91.2%	58.9%	60.7%	50.0%	65.2%

4.2 RESULTS

406 We present a detailed analysis of our experimental results across the three categories of
 407 OOD benchmarks: spurious correlation, domain shift, and subpopulation shift. The findings,
 408 summarized in Tables 1, 2, and 3, consistently demonstrate that Feature Strength
 409 Regularization (FSR) not only substantially improves OOD performance over the standard
 410 ERM baseline but also outperforms a suite of strong, SOTA methods across diverse settings.

411 **Performance on Spurious Correlation Benchmarks.** Table 1 showcases FSR’s exceptional ability
 412 to mitigate shortcut learning on datasets with strong, intentionally designed spurious correlations.
 413 On Waterbirds, FSR achieves a worst-group accuracy of **90.4%**, a near-perfect result that
 414 dramatically outperforms the next best method, Group-DRO (86.8%), and completely corrects the
 415 failure of ERM (0.0% worst-group accuracy). A key insight from these results is FSR’s ability to
 416 navigate the common trade-off between average and worst-group accuracy. Methods like IB-IRM
 417 improve worst-group performance to 85.4% but at a steep cost to average accuracy, which plummets
 418 to 64.3%. FSR, in contrast, achieves its best-in-class worst-group performance while maintaining
 419 a high average accuracy of **89.4%**, second only to ERM’s overfitted result. This suggests that
 420 FSR’s targeted intervention is more surgical, successfully weakening the model’s reliance on the
 421 spurious background feature without forcing it to discard the robust foreground features. Similarly,
 422 on CelebA, FSR improves worst-group accuracy to **78.4%**, matching Group-DRO’s performance,
 423 further validating our central hypothesis: by identifying and down-weighting the influence of the
 424 strongest spurious features, FSR guides the model toward learning more robust signals.

425 **Performance on Domain and Subpopulation Shift Benchmarks.** The effectiveness of FSR ex-
 426 tends robustly beyond synthetic correlation settings to more naturalistic domain and subpopulation
 427 shifts. As shown in Tables 2 and 3, our method demonstrates consistently superior performance.
 428 On the PACS dataset (Table 2), FSR achieves the highest average accuracy of **74.2%**, outperform-

Table 3: Results on the Digits benchmark using ResNet9 pretrained on ImageNet as backbone. Numbers are test accuracies (%). Best in **bold**.

	Digits					
	MNIST	MNISTM	SVHN	SYN	USPS	Avg.
Random Subset (50%)	87.1	63.5	55.2	76.8	81.4	72.8
CRAIG (Core-Set)	88.6	65.2	56.9	78.0	83.0	74.3
ERM	91.5	70.3	60.1	82.4	86.7	78.2
IRM	90.8	69.7	59.0	81.5	85.9	77.4
IB-IRM	92.1	71.2	61.0	83.0	87.2	78.9
Group-DRO	91.7	72.0	60.8	82.7	86.9	78.8
CORAL	92.8	71.4	62.1	83.8	87.9	79.6
FSR (Ours)	92.8	71.7	62.7	83.5	88.4	79.8

432 ing strong baselines like CORAL (73.4%) and Group-DRO (72.1%). A similar leading performance
 433 is observed on VLCS, where FSR again secures the top average accuracy (**65.2%**). This high-
 434 lights a second key insight: FSR’s principle is generalizable. Features that are statistically powerful
 435 in source domains (e.g., the “sketch” or “cartoon” artistic style) can act as spurious shortcuts that
 436 hinder generalization to an unseen target domain (e.g., “photo”). FSR’s consistent performance
 437 contrasts with the volatility of other methods; for instance, IRM’s performance on PACS (69.4%) is
 438 lower than even ERM (70.5%), suggesting its invariance principle may be less effective for complex
 439 domain shifts. Further, on the Digits benchmark (Table 3), FSR again achieves the highest average
 440 accuracy (**79.8%**), confirming its utility in handling subtle subpopulation shifts in writing styles.

441 **FSR’s Generality and Practical Advantages.** A final, crucial insight emerges when considering
 442 the practical application of FSR compared to its competitors. Across all benchmarks, FSR con-
 443 sistently outperforms naive data subsetting (Random Subset, CRAIG), confirming its benefits arise
 444 from a principled, targeted regularization rather than simple data reduction. More importantly, FSR
 445 achieves its state-of-the-art results without the stringent data requirements of other leading methods.
 446 Group-DRO, a strong competitor, requires predefined group labels, which are often unavailable in
 447 real-world datasets. Similarly, IRM necessitates data from multiple distinct training environments.
 448 FSR, however, operates on a single training distribution without needing any such annotations. By
 449 focusing on the intrinsic statistical properties of the training data itself, identifying and mitigating
 450 the influence of the strongest features, FSR provides a powerful, general, and practically accessible
 451 mechanism for improving OOD generalization. Its success across diverse distribution shifts suggests
 452 that its feature-centric perspective offers a more direct and universally applicable intervention.

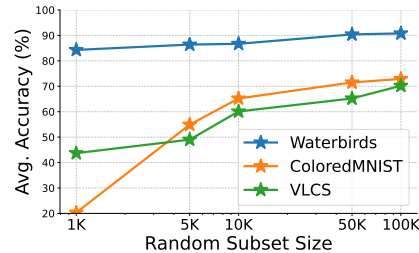
453 4.3 RUNTIME ANALYSIS

454 A critical consideration for the practical application of
 455 FSR is its computational cost. The primary expense of
 456 our method lies in the one-time, upfront computation of
 457 the datamodels, which requires training a large number
 458 of models on different subsets of the data. To analyze this
 459 cost, we investigated the relationship between the num-
 460 ber of subset models trained and the resulting accuracy
 461 of our feature strength estimation. Figure 5 illustrates
 462 this trade-off. The results show that while more subset
 463 models generally lead to higher accuracy, the gains are
 464 not linear and exhibit diminishing returns. For the Wa-
 465 terbirds dataset, performance rises sharply and begins to
 466 plateau after only 10,000 subset models, achieving over
 467 85% of its final accuracy. For more complex datasets like
 468 ColoredMNIST and VLCS, the performance continues to
 469 improve more steadily up to 50,000 models, after which
 the curve flattens considerably.

470 This analysis reveals a key practical insight: *an exhaustive computation involving an exponential*
 471 *number of subsets is not necessary to achieve strong results.* A reasonably sized sample of subset
 472 models is sufficient to obtain a reliable estimate of feature strength. Our choice of 50,000 models
 473 for the main experiments represents a practical sweet spot, balancing computational feasibility with
 474 high-quality feature strength estimation. This demonstrates that while the datamodel computation is
 475 an intensive initial step, it is a manageable and finite cost that enables the significant and consistent
 476 generalization improvements demonstrated by FSR.

477 5 CONCLUSION

478 This paper presents a new perspective on OOD generalization: failures are not just about missing
 479 invariant features, but a direct result of the learning process favoring the strongest, often spurious,
 480 signals. This reframes the challenge from seeking stable features to identifying and mitigating overly
 481 dominant ones. We proposed a novel method to quantify feature strength and regularize against
 482 the most influential training examples. Our approach improves OOD accuracy by up to 2× over
 483 standard training and significantly outperforms existing baselines without degrading in-distribution
 484 performance. Ultimately, our work suggests a shift from passively extracting invariant signals to
 485 actively managing data influences, using our feature-strength primitive as a new tool to diagnose
 and correct generalization failure.



479 **Figure 5: Impact of the number of sub-
 480 set models on FSR performance.** The plot
 481 shows the average OOD accuracy on Water-
 482 birds, ColoredMNIST, and VLCS as a func-
 483 tion of the number of models trained to com-
 484 pute the datamodels.

486 ETHICS STATEMENT
487488 We adhere to the ICLR Code of Ethics. No private, sensitive, or personally identifiable data are in-
489 volved. Our work does not raise foreseeable ethical concerns or produce harmful societal outcomes.
490491 REPRODUCIBILITY STATEMENT
492493 Reproducibility is central to our work. All datasets used in our experiments are standard benchmarks
494 that are publicly available. We provide full details of the training setup, model architectures, and
495 evaluation metrics in the main paper and appendix. Upon acceptance, we will release our codebase,
496 including scripts for preprocessing, training, and evaluation, along with configuration files and doc-
497 umentation to facilitate exact reproduction of our results. Random seeds and hyperparameters will
498 also be included to further ensure reproducibility.
499500 REFERENCES
501502 A database for handwritten text recognition research. *IEEE Transactions on pattern analysis and*
503 *machine intelligence*, 16(5):550–554, 1994.504 Kartik Ahuja, Karthikeyan Shanmugam, Kush Varshney, and Amit Dhurandhar. Invariant risk min-
505 imization games. In *International Conference on Machine Learning*, pp. 145–155. PMLR, 2020.506 Kartik Ahuja, Ethan Caballero, Dinghuai Zhang, Jean-Christophe Gagnon-Audet, Yoshua Bengio,
507 Ioannis Mitliagkas, and Irina Rish. Invariance principle meets information bottleneck for out-of-
508 distribution generalization. *Advances in Neural Information Processing Systems*, 34:3438–3450,
509 2021.510 Martin Arjovsky, Léon Bottou, Ishaan Gulrajani, and David Lopez-Paz. Invariant risk minimization.
511 *arXiv preprint arXiv:1907.02893*, 2019.512 Yogesh Balaji, Swami Sankaranarayanan, and Rama Chellappa. Metareg: Towards domain general-
513 ization using meta-regularization. In S. Bengio, H. Wallach, H. Larochelle, K. Grauman, N. Cesa-
514 Bianchi, and R. Garnett (eds.), *Advances in Neural Information Processing Systems*, volume 31.
515 Curran Associates, Inc., 2018. URL https://proceedings.neurips.cc/paper_files/paper/2018/file/647bba344396e7c8170902bcf2e15551-Paper.pdf.516 Sara Beery, Grant Van Horn, and Pietro Perona. Recognition in terra incognita. In *Proceedings of*
517 *the European conference on computer vision (ECCV)*, pp. 456–473, 2018.518 Shai Ben-David, John Blitzer, Koby Crammer, Alex Kulesza, Fernando C Pereira, and Jen-
519 nifer Wortman Vaughan. A theory of learning from different domains. *Machine Learning*, 79:
520 151–175, 2010. URL <https://api.semanticscholar.org/CorpusID:8577357>.521 Yoshua Bengio, Tristan Deleu, Nasim Rahaman, Rosemary Ke, Sébastien Lachapelle, Olexa Bila-
522 niuk, Anirudh Goyal, and Christopher Pal. A meta-transfer objective for learning to disentangle
523 causal mechanisms. *arXiv preprint arXiv:1901.10912*, 2019.524 Anwesha Bhattacharyya, Yaqun Wang, Joel Vaughan, and Vijayan N Nair. Using markov boundary
525 approach for interpretable and generalizable feature selection. *arXiv preprint arXiv:2307.14327*,
526 2023.527 Liang Chen, Yong Zhang, Yibing Song, Zhen Zhang, and Lingqiao Liu. A causal inspired early-
528 branching structure for domain generalization. *International Journal of Computer Vision*, 132(9):
529 4052–4072, 2024.530 Alex J. DeGrave, Joseph D. Janizek, and Su-In Lee. Ai for radiographic covid-19 detection selects
531 shortcuts over signal. *medRxiv*, 2020. doi: 10.1101/2020.09.13.20193565. URL <https://www.medrxiv.org/content/early/2020/09/14/2020.09.13.20193565>.532 Jia Deng, Wei Dong, Richard Socher, Li-Jia Li, Kai Li, and Li Fei-Fei. Imagenet: A large-scale hier-
533 archical image database. In *2009 IEEE Conference on Computer Vision and Pattern Recognition*,
534 pp. 248–255, 2009. doi: 10.1109/CVPR.2009.5206848.

540 Chelsea Finn, Pieter Abbeel, and Sergey Levine. Model-agnostic meta-learning for fast adaptation
 541 of deep networks. In *International conference on machine learning*, pp. 1126–1135. PMLR, 2017.
 542

543 Yaroslav Ganin, Evgeniya Ustinova, Hana Ajakan, Pascal Germain, Hugo Larochelle, François
 544 Laviolette, Mario March, and Victor Lempitsky. Domain-adversarial training of neural networks.
 545 *Journal of machine learning research*, 17(59):1–35, 2016.

546 Robert Geirhos, Jörn-Henrik Jacobsen, Claudio Michaelis, Richard Zemel, Wieland Brendel,
 547 Matthias Bethge, and Felix A Wichmann. Shortcut learning in deep neural networks. *Nature
 548 Machine Intelligence*, 2(11):665–673, 2020.

549 Kaiming He, Xiangyu Zhang, Shaoqing Ren, and Jian Sun. Deep residual learning for image recog-
 550 nition. In *Proceedings of the IEEE conference on computer vision and pattern recognition*, pp.
 551 770–778, 2016.

552 Christina Heinze-Deml, Jonas Peters, and Nicolai Meinshausen. Invariant causal prediction for
 553 nonlinear models. *Journal of Causal Inference*, 6(2):20170016, 2018.

554 Andrew Ilyas, Sung Min Park, Logan Engstrom, Guillaume Leclerc, and Aleksander Madry. Data-
 555 models: Predicting predictions from training data. *arXiv preprint arXiv:2202.00622*, 2022.

556 Liangze Jiang and Damien Teney. Ood-chameleon: Is algorithm selection for ood generalization
 557 learnable? *arXiv preprint arXiv:2410.02735*, 2024.

558 B. W. Kernighan and S. Lin. An efficient heuristic procedure for partitioning graphs. *The Bell
 559 System Technical Journal*, 49(2):291–307, 1970. doi: 10.1002/j.1538-7305.1970.tb01770.x.

560 Alaa Khaddaj, Guillaume Leclerc, Aleksandar Makelov, Kristian Georgiev, Hadi Salman, Andrew
 561 Ilyas, and Aleksander Madry. Rethinking backdoor attacks. In *International Conference on
 562 Machine Learning*, pp. 16216–16236. PMLR, 2023.

563 Diederik P Kingma and Jimmy Ba. Adam: A method for stochastic optimization. *arXiv preprint
 564 arXiv:1412.6980*, 2014.

565 Masanori Koyama and Shoichiro Yamaguchi. When is invariance useful in an out-of-distribution
 566 generalization problem? *arXiv preprint arXiv:2008.01883*, 2020.

567 Alex Krizhevsky. Learning multiple layers of features from tiny images. 2009. URL <https://api.semanticscholar.org/CorpusID:18268744>.

568 David Krueger, Ethan Caballero, Joern-Henrik Jacobsen, Amy Zhang, Jonathan Binas, Dinghuai
 569 Zhang, Remi Le Priol, and Aaron Courville. Out-of-distribution generalization via risk extrapo-
 570 lation (rex). In *International conference on machine learning*, pp. 5815–5826. PMLR, 2021.

571 Y. Lecun, L. Bottou, Y. Bengio, and P. Haffner. Gradient-based learning applied to document recog-
 572 nition. *Proceedings of the IEEE*, 86(11):2278–2324, 1998. doi: 10.1109/5.726791.

573 Da Li, Yongxin Yang, Yi-Zhe Song, and Timothy M Hospedales. Deeper, broader and artier domain
 574 generalization. In *Proceedings of the IEEE international conference on computer vision*, pp.
 575 5542–5550, 2017.

576 Haoliang Li, Sinno Jialin Pan, Shiqi Wang, and Alex Chichung Kot. Domain generalization with
 577 adversarial feature learning. *2018 IEEE/CVF Conference on Computer Vision and Pattern Recog-
 578 nition*, pp. 5400–5409, 2018. URL [https://api.semanticscholar.org/CorpusID:
 579 52833113](https://api.semanticscholar.org/CorpusID:52833113).

580 Jiashuo Liu, Zheyan Shen, Yue He, Xingxuan Zhang, Renzhe Xu, Han Yu, and Peng Cui. Towards
 581 out-of-distribution generalization: A survey. *arXiv preprint arXiv:2108.13624*, 2021.

582 Ziwei Liu, Ping Luo, Xiaogang Wang, and Xiaoou Tang. Deep learning face attributes in the wild.
 583 In *Proceedings of International Conference on Computer Vision (ICCV)*, December 2015.

584 Baharan Mirzasoleiman, Jeff Bilmes, and Jure Leskovec. Coresets for data-efficient training of
 585 machine learning models. In *International Conference on Machine Learning*, pp. 6950–6960.
 586 PMLR, 2020.

594 Peyman Mohajerin Esfahani and Daniel Kuhn. Data-driven distributionally robust optimization
 595 using the wasserstein metric: Performance guarantees and tractable reformulations. *Mathematical*
 596 *Programming*, 171(1):115–166, 2018.

597

598 Jose G. Moreno-Torres, Troy Raeder, Rocío Alaiz-Rodríguez, Nitesh V. Chawla, and Francisco
 599 Herrera. A unifying view on dataset shift in classification. *Pattern Recognition*, 45(1):521–
 600 530, 2012. ISSN 0031-3203. doi: <https://doi.org/10.1016/j.patcog.2011.06.019>. URL <https://www.sciencedirect.com/science/article/pii/S0031320311002901>.

601

602 Yuval Netzer, Tao Wang, Adam Coates, A. Bissacco, Bo Wu, and A. Ng. Reading digits in natural
 603 images with unsupervised feature learning. 2011. URL <https://api.semanticscholar.org/CorpusID:16852518>.

604

605 Xingchao Peng, Qinxun Bai, Xide Xia, Zijun Huang, Kate Saenko, and Bo Wang. Moment matching
 606 for multi-source domain adaptation. In *Proceedings of the IEEE/CVF International Conference*
 607 *on Computer Vision (ICCV)*, October 2019.

608

609 Jonas Peters, Peter Bühlmann, and Nicolai Meinshausen. Causal inference by using invariant pre-
 610 diction: identification and confidence intervals. *Journal of the Royal Statistical Society Series B: Statistical Methodology*, 78(5):947–1012, 2016.

611

612 Mohammad Pezeshki, Oumar Kaba, Yoshua Bengio, Aaron C Courville, Doina Precup, and Guillaume
 613 Lajoie. Gradient starvation: A learning proclivity in neural networks. *Advances in Neural*
 614 *Information Processing Systems*, 34:1256–1272, 2021.

615

616 Benjamin Recht, Rebecca Roelofs, Ludwig Schmidt, and Vaishaal Shankar. Do imagenet classifiers
 617 generalize to imagenet? In *International conference on machine learning*, pp. 5389–5400. PMLR,
 618 2019.

619

620 Alexander Robey, George J Pappas, and Hamed Hassani. Model-based domain generalization. *Advances*
 621 *in Neural Information Processing Systems*, 34:20210–20229, 2021.

622

623 Mateo Rojas-Carulla, Bernhard Schölkopf, Richard Turner, and Jonas Peters. Invariant models for
 624 causal transfer learning. *Journal of Machine Learning Research*, 19(36):1–34, 2018.

625

626 Shiori Sagawa, Pang Wei Koh, Tatsunori B Hashimoto, and Percy Liang. Distributionally robust
 627 neural networks for group shifts: On the importance of regularization for worst-case generaliza-
 628 tion. *arXiv preprint arXiv:1911.08731*, 2019.

629

630 Shiori Sagawa, Pang Wei Koh, Tatsunori B. Hashimoto, and Percy Liang. Distributionally robust
 631 neural networks. In *International Conference on Learning Representations*, 2020. URL <https://openreview.net/forum?id=ryxGuJrFvS>.

632

633 Baochen Sun and Kate Saenko. Deep coral: Correlation alignment for deep domain adaptation. In
 634 *European conference on computer vision*, pp. 443–450. Springer, 2016.

635

636 Rohan Taori, Achal Dave, Vaishaal Shankar, Nicholas Carlini, Benjamin Recht, and Ludwig
 637 Schmidt. Measuring robustness to natural distribution shifts in image classification. *Advances*
 638 *in Neural Information Processing Systems*, 33:18583–18599, 2020.

639

640 Antonio Torralba and Alexei A. Efros. Unbiased look at dataset bias. *CVPR 2011*, pp. 1521–1528,
 641 2011. URL <https://api.semanticscholar.org/CorpusID:2777306>.

642

643 Vladimir Naumovich Vapnik. Principles of risk minimization for learning theory. In *Neural*
 644 *Information Processing Systems*, 1991. URL <https://api.semanticscholar.org/CorpusID:15348764>.

645

646 C. Wah, S. Branson, P. Welinder, P. Perona, and S. Belongie. Caltech birds dataset. Technical report,
 647 2011.

648

649 Dinghuai Zhang, Kartik Ahuja, Yilun Xu, Yisen Wang, and Aaron Courville. Can subnetwork
 650 structure be the key to out-of-distribution generalization? In *International conference on machine*
 651 *learning*, pp. 12356–12367. PMLR, 2021a.

648 Jiayuan Zhang, Xuefeng Liu, Jianwei Niu, Shaojie Tang, Haotian Yang, and Xinghao Wu. Causality
 649 inspired federated learning for OOD generalization. In *Forty-second International Conference on*
 650 *Machine Learning*, 2025. URL <https://openreview.net/forum?id=pWWUJw2qew>.

651

652 Xingxuan Zhang, Peng Cui, Renzhe Xu, Linjun Zhou, Yue He, and Zheyuan Shen. Deep stable
 653 learning for out-of-distribution generalization. In *Proceedings of the IEEE/CVF conference on*
 654 *computer vision and pattern recognition*, pp. 5372–5382, 2021b.

655 Shanshan Zhao, Mingming Gong, Tongliang Liu, Huan Fu, and Dacheng Tao. Domain generaliza-
 656 tion via entropy regularization. In H. Larochelle, M. Ranzato, R. Hadsell, M.F. Balcan, and H. Lin
 657 (eds.), *Advances in Neural Information Processing Systems*, volume 33, pp. 16096–16107. Cur-
 658 ran Associates, Inc., 2020. URL https://proceedings.neurips.cc/paper_files/paper/2020/file/b98249b38337c5088bbc660d8f872d6a-Paper.pdf.

659

660 Bolei Zhou, Agata Lapedriza, Jianxiong Xiao, Antonio Torralba, and Aude Oliva. Learning deep features for scene recognition using places database. In Z. Ghahramani,
 661 M. Welling, C. Cortes, N. Lawrence, and K.Q. Weinberger (eds.), *Advances in Neu-*
 662 *ral Information Processing Systems*, volume 27. Curran Associates, Inc., 2014. URL
 663 https://proceedings.neurips.cc/paper_files/paper/2014/file/19ea3982b415d7bb3363917eb3d60c4a-Paper.pdf.

664

665

666

667

A LLM USAGE

670 To enhance clarity and readability, we utilized LLMs (specifically OpenAI GPT-4o) exclusively
 671 as a language polishing tool. Its role was confined to proofreading, grammatical correction, and
 672 stylistic refinement—functions analogous to those provided by traditional grammar checkers and
 673 dictionaries. This tool did not contribute to the generation of new scientific content or ideas, and its
 674 usage is consistent with standard practices for manuscript preparation.

B EXTENDED RELATED WORKS

675 Methods such as Domain-Adversarial Neural Network (DANN) (Ganin et al., 2016) approach the
 676 problem by learning representations that are indistinguishable across domains. A domain classifier
 677 is trained to predict the source domain of a feature representation, while the feature extractor is
 678 trained to fool this classifier, thus encouraging domain-invariant features. This adversarial approach
 679 has inspired a range of methods that aim to align feature distributions across domains (Li et al.,
 680 2018; Zhao et al., 2020). Our method, in contrast, does not require multiple domains and operates
 681 on a different principle: it identifies features that are overly influential within a single training set
 682 and mitigates their dominance, assuming that extreme statistical strength is a proxy for being a
 683 spurious shortcut. Other techniques leverage meta-learning, such as Model-Agnostic Meta-Learning
 684 (MAML) adapted for domain generalization (Finn et al., 2017). These methods simulate domain
 685 shift during training by partitioning source domains into meta-train and meta-test sets, aiming to
 686 learn an optimization procedure that generalizes well to new tasks or domains (Chen et al., 2024;
 687 Balaji et al., 2018). Finally, some approaches explicitly model the data generation process. Causal
 688 learning methods, such as Invariant Causal Prediction (Peters et al., 2016), attempt to learn the
 689 underlying causal graph of the data, to make predictions based only on the direct causes of the label,
 690 which are assumed to be invariant (Rojas-Carulla et al., 2018; Heinze-Deml et al., 2018). Our work
 691 provides a different diagnostic tool: we assume that the failure to learn these stable mechanisms is
 692 due to the overwhelming influence of the strongest spurious features. Our primitive for quantifying
 693 feature strength offers a direct way to identify and intervene against these dominant signals.

694 The common assumption for feature selection is that a truly robust model should only depend on
 695 this causally sufficient set. However, these approaches typically require strong prior knowledge or
 696 access to multiple training environments to perform the necessary conditional independence tests
 697 for identifying the causal structure. Our work offers an alternative path: instead of trying to identify
 698 the causal graph, we provide a mechanism to quantify the statistical influence of any feature on
 699 the learned model. We operate under a different assumption: that the strongest features are the
 700 most likely to be spurious shortcuts. This reframes the problem from a search for a pre-defined

702 set of “correct” features to an intervention against the most empirically dominant ones, providing a
 703 practical heuristic when clear causal information is unavailable.
 704

705 **C PROOF OF THEOREM 1**

706 **Assumptions.**

707 • **Assumption 1 (Strongest Feature Hypothesis).** Let c_s be a spurious feature and c_r a robust
 708 causal feature. In a biased training set, the spurious feature is statistically stronger, i.e., $I_{c_s}(k) >$
 709 $I_{c_r}(k)$ for relevant values of k . An ERM-trained model will thus preferentially learn c_s at the
 710 expense of c_r .

711 • **Assumption 2 (Datamodel Accuracy).** For any test example z with datamodel weight vector
 712 $w_z \in \mathbb{R}^n$, the expected squared error of the datamodel approximation is bounded:

$$713 \mathbb{E}_{S' \sim \mathcal{D}_S} \left[(\mathbb{E}[f(z; S')] - \mathbb{1}_{S'}^T w_z)^2 \right] \leq \epsilon,$$

714 ensuring datamodel-based estimates reliably approximate feature influence.

715 **Theorem 1 (Feature Identification).** Let c_p be the strongest feature in the dataset with support size
 716 p . Under Assumptions 1 and 2, if the strength gap between c_p and any other feature is sufficiently
 717 large, the unique maximizer of the quadratic optimization problem is the indicator vector $v_p = \mathbb{1}_{S_{c_p}}$
 718 corresponding to the support set of c_p .

719 **Proof.** Let c_p be the strongest feature with support S_{c_p} of size p , and $v_p = \mathbb{1}_{S_{c_p}}$. For any other
 720 feature c with support S_c (also of size p), define $v_c = \mathbb{1}_{S_c}$. We contrast the influence of examples
 721 inside and outside a candidate support using

$$722 h(v) = \frac{1}{\|v\|_1} v - \frac{1}{n - \|v\|_1} (1_n - v).$$

723 The optimization problem seeks the maximizer of $J(v) = h(v)^T W v$, where W is the datamodel
 724 influence matrix.

725 The true marginal influence of a feature c on a test example z is

$$726 I_c(z, k) = V_c(z, k+1) - V_c(z, k),$$

727 but this is computationally intractable. By Assumption 2, we use the datamodel approximation:

$$728 \mathbb{E}[f(z; S')] \approx \mathbb{1}_{S'}^T w_z.$$

729 Thus, the estimated marginal influence is

$$730 \hat{I}_c(z, k) = \mathbb{E}_{S'} [\mathbb{1}_{S'}^T w_z \mid \|S'\| = k+1] - \mathbb{E}_{S'} [\mathbb{1}_{S'}^T w_z \mid \|S'\| = k].$$

731 Under uniform sampling of subsets, this reduces to

$$732 \hat{I}_c(z, k) = \frac{1}{p} \sum_{i \in S_c} w_{zi} - \frac{1}{n-p} \sum_{j \notin S_c} w_{zj} = w_z^T h(v_c).$$

733 Let $\bar{I}_c(k)$ be the true average marginal influence and \hat{I}_c its datamodel-based estimate:

$$734 \hat{I}_c = \frac{1}{p} \sum_{z \in S_c} w_z^T h(v_c).$$

735 By Lemma 1 of [Khaddaj et al. \(2023\)](#), the approximation error is bounded:

$$736 |\bar{I}_c(k) - \hat{I}_c| \leq \epsilon_{\text{approx}} \quad \text{where} \quad \epsilon_{\text{approx}} = C\epsilon^{1/2}n^{1/4}.$$

737 Since $J(v_c) = h(v_c)^T W v_c \approx p \cdot \hat{I}_c$, we have

$$738 J(v_p) \geq p(\bar{I}_{c_p} - \epsilon_{\text{approx}}), \quad J(v_c) \leq p(\bar{I}_c + \epsilon_{\text{approx}}).$$

739 By Assumption 1, there exists $\delta > 0$ such that $\bar{I}_{c_p} \geq \bar{I}_c + \delta$. Hence

$$740 J(v_p) - J(v_c) \gtrsim p(\delta - 2\epsilon_{\text{approx}}).$$

741 If $\delta > 2\epsilon_{\text{approx}}$, then $J(v_p) > J(v_c)$ for all $v_c \neq v_p$. Therefore, v_p is the unique maximizer. ■

756 **D PROOF OF THEOREM 2**
757758 **Assumptions.**
759

760 • **Assumption 1 (Strongest Feature Hypothesis).** Defined as in Theorem 1.
 761 • **Assumption 2 (Datamodel Accuracy).** Defined as in Theorem 1.
 762 • **Assumption 3 (Feature Decomposition).** The predictor f_θ can be decomposed into contributions
 763 from the strongest spurious feature c_s , the robust feature c_r , and residual terms:

764
$$f_\theta(x) = \theta_s c_s(x) + \theta_r c_r(x) + f_{\text{rest}}(x).$$

 765

766 **Theorem 2 (Generalization Improvement of FSR over ERM).** Let c_s be the strongest spurious
 767 feature (its correlation with y changes between P_{tr} and P_{te}), and c_r a weaker but robust feature
 768 (its correlation with y remains stable). Under Assumptions 1–3, the expected OOD risk of FSR is
 769 strictly lower than that of ERM:

770
$$\mathbb{E}_{P_{te}}[\mathcal{L}_{FSR}] < \mathbb{E}_{P_{te}}[\mathcal{L}_{ERM}].$$

 771

772 **Proof.** Under ERM, the learned parameter vector θ_{ERM} minimizes
 773

774
$$\theta_{ERM} = \arg \min_{\theta} \mathbb{E}_{(x,y) \sim P_{tr}} [\mathcal{L}(f_\theta(x), y)].$$

 775

776 By Assumption 1, c_s is the statistically strongest signal in P_{tr} , so $\theta_{s,ERM}$ is large. Thus, $f_{\theta_{ERM}}$
 777 over-relies on c_s , while $\theta_{r,ERM}$ remains small. On the shifted distribution P_{te} , the spurious corre-
 778 lation breaks, so

779
$$R_{te}(f_{\theta_{ERM}}) = \mathbb{E}_{(x,y) \sim P_{te}} [\mathcal{L}(f_{\theta_{ERM}}(x), y)]$$

780 is high due to systematic errors induced by $\theta_{s,ERM}$.

781 In contrast, FSR solves

782
$$\theta_{FSR} = \arg \min_{\theta} \frac{1}{n} \sum_{i=1}^n \lambda_i \mathcal{L}(f_\theta(x_i), y_i),$$

 783

784 where λ_i downweights samples in S_{c_s} . This reduces the incentive to fit c_s , yielding $|\theta_{s,FSR}| <$
 785 $|\theta_{s,ERM}|$ and comparatively larger $|\theta_{r,FSR}|$. On P_{te} , this shift mitigates the contribution of the
 786 spurious c_s while enhancing reliance on the robust c_r , giving

787
$$R_{te}(f_{\theta_{FSR}}) < R_{te}(f_{\theta_{ERM}}).$$

 788

789 Thus, the expected OOD risk of FSR is strictly lower than ERM’s. ■
 790

791 **E DATASET DESCRIPTIONS**
792

793 In this section, we provide detailed descriptions of the datasets used in our experiments.

794 **Waterbirds.** The Waterbirds dataset (Sagawa et al., 2020) is a standard benchmark for evaluating
 795 spurious correlations. It is a binary classification task designed to distinguish “water birds” from
 796 “land birds”. The dataset is constructed by combining images of birds from the Caltech-UCSD
 797 Birds-200-2011 (CUB) dataset (Wah et al., 2011) with backgrounds from the Places dataset Zhou
 798 et al. (2014). A strong spurious correlation is introduced: in the training set, water birds are predom-
 799 inantly shown on water backgrounds (95% correlation), and land birds are predominantly shown
 800 on land backgrounds (95% correlation). The test set contains examples from all four combinations
 801 (water bird/water background, water bird/land background, etc.), with a significant portion of exam-
 802 ples belonging to the minority groups (e.g., water birds on land). The model’s ability to generalize
 803 is measured by its worst-group accuracy on these minority combinations.

804 **Colored MNIST.** Colored MNIST (Arjovsky et al., 2019) is a synthetic dataset created from the
 805 original MNIST dataset of handwritten digits (Lecun et al., 1998). It introduces a spurious corre-
 806 lation between digit color and class label. For the binary classification task (digits 0 – 4 vs. 5 – 9),
 807 a color (e.g., red or green) is assigned to each digit with a high probability that correlates with the
 808 label in the training set (e.g., 90% of digits < 5 are red, 90% of digits ≥ 5 are green). In the test set,
 809 this correlation is reversed, forcing the model to rely on the digit’s shape rather than its color.

CelebA. The CelebA dataset (Liu et al., 2015) is a large-scale dataset of celebrity face attributes. For OOD generalization tasks, it is commonly used to study spurious correlations between facial attributes. In our experiments, we use it for a binary classification task, such as predicting hair color (“blond” vs. “not blond”), where a spurious correlation with gender (“male” vs. “female”) is present. The training data is highly imbalanced, with certain attribute combinations (e.g., “blond” and “male”) being significantly underrepresented. Performance is evaluated based on worst-group accuracy across the four attribute combinations.

PACS. PACS (Li et al., 2017) consists of images from four distinct domains: Photo, Art Painting, Cartoon, and Sketch, across 7 object categories.

VLCS. VLCS (Torralba & Efros, 2011) combines images from four datasets: Pascal VOC2007, LabelMe, Caltech-101, and SUN09, covering 5 common object classes.

For these two datasets, we follow the standard “leave-one-domain-out” protocol. The model is trained on data from all but one domain, and then evaluated on the held-out, unseen domain. This process is repeated for each domain, and the average accuracy across held-out domains is reported.

Digits. The Digits benchmark is a collection of several handwritten digit datasets, including MNIST (Lecun et al., 1998), SVHN (Netzer et al., 2011), and USPS (hul, 1994). Each dataset is treated as a separate domain, exhibiting shifts in style, font, image resolution, and background. Similar to the other domain shift benchmarks, we use a leave-one-domain-out evaluation strategy.

F BASELINE DESCRIPTIONS

In this section, we provide brief descriptions of the baseline methods used for comparison in our experiments.

Random Subset. This is a simple data selection baseline where the model is trained on a randomly selected subset (e.g., 50%) of the training data. It serves to evaluate the impact of data reduction alone, isolating it from the effect of an intelligent selection strategy.

CRAIG (Core-Set). This method (Mirzaoleiman et al., 2020) provides a more sophisticated data selection baseline. It is a core-set selection algorithm that greedily identifies a small, representative subset of the training data that is most informative for the learning task. Training on this core-set can improve efficiency and sometimes generalization by focusing on the most valuable examples.

Empirical Risk Minimization (ERM). This is the standard and most fundamental baseline in supervised learning (Vapnik, 1991). The ERM algorithm trains the model by minimizing the average loss computed over the entire training dataset. It does not incorporate any specific mechanism to address distribution shifts and thus serves as the primary reference for measuring the effectiveness of OOD generalization methods.

Invariant Risk Minimization (IRM). IRM is a foundational approach for OOD generalization that aims to learn an invariant predictor across multiple training environments (Arjovsky et al., 2019). The core idea is to find a data representation for which the optimal classifier is the same across all observed domains. This is intended to force the model to learn causal features rather than relying on spurious correlations that are environment-specific. This method requires the training data to be partitioned into multiple distinct domains.

Information Bottleneck IRM (IB-IRM). This method (Ahuja et al., 2021) applies a regularization term inspired by the Information Bottleneck principle to the standard IRM objective. The goal is to learn a representation that is maximally compressive with respect to the input while retaining sufficient information for the prediction task. By penalizing model complexity in this way, IB-IRM encourages the model to discard non-essential, and often spurious, features, which can improve robustness to distribution shifts.

Group Distributionally Robust Optimization (Group-DRO). Group-DRO (Sagawa et al., 2020) is an algorithm designed to improve worst-case performance over predefined groups within the training data. It explicitly minimizes the risk on the group with the highest error, which is achieved by adaptively increasing the weights of examples from under-performing groups during training. This makes the model more robust to subpopulation shifts, particularly those affecting minority groups. This method requires explicit group annotations for the training data.

864 **Correlation Alignment (CORAL)** CORAL (Sun & Saenko, 2016) is a domain adaptation method
865 often adapted as a baseline for domain generalization. It aims to learn a domain-invariant feature
866 representation by minimizing the difference between the second-order statistics (i.e., the covariance)
867 of the source domain distributions. By adding a penalty term that encourages the alignment of these
868 covariances, CORAL discourages the model from learning domain-specific features.
869

870 G IMPLEMENTATION DETAILS. 871

872 For the datamodel computation, a one-time upfront cost, we train 50,000 ResNet-9 models on ran-
873 dom 50% subsets of the training data. For FSR, the regularization weights λ_i are determined by the
874 feature strength scores, where we rank the examples and apply a linear decay to the weights of the
875 top 10% strongest examples. All models are trained using the Adam (Kingma & Ba, 2014) with a
876 learning rate of 1e-3 and a batch size of 128. Furthermore, all experiments are repeated 3 times with
877 different seeds.
878
879
880
881
882
883
884
885
886
887
888
889
890
891
892
893
894
895
896
897
898
899
900
901
902
903
904
905
906
907
908
909
910
911
912
913
914
915
916
917